PHYSICAL REVIEW A **87**, 030301(R) (2013)

Process verification of two-qubit quantum gates by randomized benchmarking

A. D. Córcoles,[1] Jay M. Gambetta,[1] Jerry M. Chow,[1] John A. Smolin,[1] Matthew Ware,[2] Joel Strand,[2] B. L. T. Plourde,[2] and M. Steffen[1]

[1]*IBM T.J. Watson Research Center, Yorktown Heights, New York 10598, USA*

[2]*Department of Physics, Syracuse University, Syracuse, New York 13244, USA*

(Received 24 October 2012; published 19 March 2013)

We implement a complete randomized benchmarking protocol on a system of two superconducting qubits. The protocol consists of randomizing over gates in the Clifford group, which experimentally are generated via an improved two-qubit cross-resonance gate implementation and single-qubit unitaries. From this we extract an optimal average error per Clifford operation of 0.0936. We also perform an interleaved experiment, alternating our optimal two-qubit gate with random two-qubit Clifford gates, to obtain a two-qubit gate error of 0.0653. We compare these values with a two-qubit gate error of ∼0.12 obtained from quantum process tomography, which is likely limited by state preparation and measurement errors.

DOI: 10.1103/PhysRevA.87.030301 PACS number(s): 03.67.Ac, 03.67.Lx, 42.50.Pq, 85.25.−j

A task of fundamental importance in the development of large-scale quantum processors is that of determining a robust, multiplatform standard to quantify the quality of the quantum operations. Characterizing quantum gates becomes harder as the error of the gates continues to decrease. The standard method of quantum process tomography [1,2] (QPT) gives a full description of the protocol under study, but is very sensitive to state preparation and measurement (SPAM) errors. As an alternative, recent work has been devoted to the development of randomized benchmarking (RB) protocols [3–5], which have been implemented in ion traps [4,6,7], NMR [8], superconducting qubits [9–11], and atoms in optical lattices [12]. Although a RB protocol offers a reliable estimate of the average error per operator within a group of operators in its original conception, it does not provide a complete description of a given quantum process. However, recent studies [13,14] have presented a different RB implementation to circumvent this problem. Furthermore, RB has also been used to determine addressability errors and correlations in many-body quantum systems [15].

In this paper, we present a complete RB characterization of two fixed-frequency superconducting qubits, achieved via a robust all-microwave two-qubit gate which is calibrated and inserted into sequences of arbitrary length on demand. This experimental realization of two-qubit RB on superconducting qubits clears a significant hurdle of implementing long sequences of two-qubit gates, as would be the case in a real quantum algorithm. The two-qubit gate used in the realization of our RB protocol is made possible by modifying a previously developed cross-resonance (CR) two-qubit interaction [16,17] through refocusing the single-qubit dynamics to simplify the gate calibration. This modified pulse sequence is reminiscent of multiqubit Hamiltonian decoupling control sequences pioneered in NMR qubit systems [18], and further reflects the importance of optimizing quantum control protocols for larger-scale quantum computations.

Our implementation of the RB protocol is restricted to the Clifford (Cl) group $\mathcal{C}$ of operators, which is the normalizer of the Pauli group $\mathcal{P}$—that is, for each $C \in \mathcal{C}$, $CPC^\dagger \in \mathcal{P}$, with $P \in \mathcal{P}$. A Cl-based RB protocol is readily extendable to systems with a high number of qubits, as choosing a random Cl element and decomposing it into a set of generators (elementary qubit operations) scales polynomially in the number of qubits [5,19]. Besides, as the set of generators tends to vary across systems, such a protocol offers portability between the different physical implementations of quantum processors.

The two-qubit Cl group is generated from single-qubit unitaries and a controlled-NOT (CNOT) gate. When implementing the protocol, it is important to use a Cl decomposition into elementary unitaries that minimizes the number of average two-qubit gates per Cl operation, as these tend to have lower fidelities than single-qubit gates, especially in the case of superconducting qubits. In contrast to Ref. [5], to generate a random Cl operation here we use an optimized set of Cl operations from which we randomly select elements. We divided the two-qubit Cl group into four classes [20]: a class with 576 elements containing only single-qubit unitaries from the group $\{I, X_{\pm\pi/2}, Y_{\pm\pi/2}, X_\pi, Y_\pi\}$, where U_θ represents a rotation of angle θ around the axis U; two classes with 5184 elements each containing single-qubit unitaries and either one or two CNOT gates; and a class with 576 elements containing single-qubit unitaries and a SWAP gate, implemented by three CNOT gates. Therefore, the total number of elements in the two-qubit Cl group is 11 520, with an average of 1.5 CNOT gates per Cl operation [21].

The experiments are performed on two single-junction transmons coupled via a superconducting coplanar waveguide resonator, which is also used for readout [22]. The qubit resonance frequencies are $\omega_1/2\pi = 3.2324$ and $\omega_2/2\pi = 3.2945$ GHz, whereas the bare resonator frequency is $\omega_r/2\pi = 8.2855$ GHz. The energy relaxation times of both qubits are observed to be $T_1^{(1)} = 11.6$ μs and $T_1^{(2)} = 9.1$ μs, and the coherence times observed from echo experiments are $T_2^{(1)} = 17.8$ μs and $T_2^{(2)} = 6.4$ μs [20]. The qubits are thermally anchored to the coldest stage of a dilution refrigerator with a nominal base temperature of 15 mK and are carefully shielded against thermal radiation [23,24].

Implementing the Cl group of operators in our experiments required modifying a previously demonstrated two-qubit CR gate [16]. The basis of the original CR gate [25,26] involves the driving of the control qubit at the frequency of the target

qubit. This results in a driving Hamiltonian of the form

$$H_D/\hbar \approx \epsilon(t)(mIX - \mu ZX + \eta ZI), \quad (1)$$

where $\{I,X,Y,Z\}^{\otimes 2}$ are the two-qubit Pauli operators, $\epsilon/2\pi$ is the drive amplitude in Hz, μ is a coupling parameter that equals J/Δ for ideal qubits, where J is the qubit-qubit coupling energy and Δ is the frequency detuning between the qubits, m is a scalar representing the effect of spurious electromagnetic crosstalk between both qubits as well as the effect of higher energy levels, and η represents the magnitude of the Stark shift arising from the off-resonant driving of qubit 1. The term mIX results in Rabi-like oscillations of qubit 2, to which the term $-\mu ZX$ contributes with a slower rotation whose sign depends on the state of qubit 1. The effect of the Hamiltonian H_D can be seen in the experiments shown in Fig. 1(a). A CR pulse of total variable length τ_1, shaped as a half-Gaussian turn-on and -off (Gaussian half-length = 24 ns, Gaussian σ = 8 ns) in order to ensure adiabaticity, is applied to qubit 1 (control) at the frequency of qubit 2 (target). Depending on whether a π rotation is applied to qubit 1 prior to the CR pulse (circles) or not (triangles), different Rabi rates are observed on qubit 2. In the experiments in which qubit 1 is in the excited state prior to the CR pulse, an additional π rotation is applied to qubit 1 at the end of the sequence in order to return it to its ground state before readout. All single-qubit rotations are Gaussian-shaped pulses with Gaussian width σ = 8 ns and total length 4σ = 32 ns. All π rotations shown in Fig. 1 are around the x axis. All single-qubit pulses include a calibrated derivative in the other quadrature [9,27].

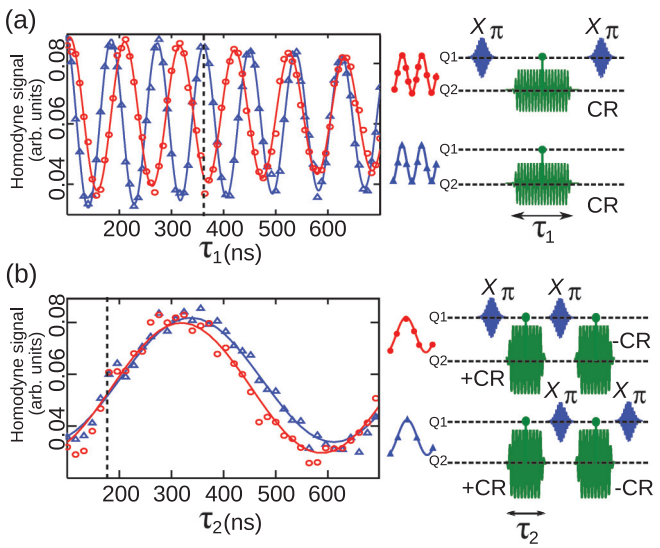

FIG. 1. (Color online) Homodyne signal as a function of the cross-resonance tone length and pulse sequences for the standard cross-resonance gate (a) and for the $ZX_{-\pi/2}$ (b). All tones are applied to the control qubit driving line (Q1), with the π pulses and cross-resonance tones applied at the control and target qubit frequencies, respectively. The system is in its ground state at the beginning of each sequence. The π pulse between the two cross-resonance tones in the $ZX_{-\pi/2}$ gate, along with the opposite sign of the second cross-resonance pulse, echo away the fast IX component of the driving Hamiltonian seen in (a) and leave only the ZX interaction. The dashed vertical lines mark the half-gate length used for the RB experiments for the $ZX_{-\pi/2}$ gate and the equivalent length for the standard cross-resonance gate.

The Hamiltonian in Eq. (1), however, presents difficulties for implementing long sequences of Cl gates due to the single-qubit terms. These terms could be explicitly tuned out with additional simultaneous pulses, but this would be rather demanding on the phase-locking and amplitude stability requirements of the electronics and on sequence complexity which would have an important negative impact on the gate fidelity. Instead, we construct a more manageable two-qubit Cl gate by modifying the original pulse sequence in order to remove all terms except ZX. The new pulse sequence divides the CR pulse in three parts: an initial CR pulse of duration τ_2, a π rotation of qubit 1, and a final CR pulse of opposite sign to the first one, also of duration τ_2. As in the original pulse scheme, a final π rotation is applied to qubit 1 when pertinent. The net effect of the new pulse sequence is to effectively "echo" away IX and ZI in H_D and, as a result, only the slower Rabi-rotation arising from ZX is observed [Fig. 1(b)]. In both Figs. 1(a) and 1(b), the system is in its ground state at the beginning of each pulse sequence. In the experiments presented here, the gate is realized by choosing a value of τ_2 that leaves qubit 2 in a superposition of $|0\rangle$ and $|1\rangle$. We will therefore call this gate $ZX_{-\pi/2}$, the minus sign arising from the negative term involving ZX in Eq. (1). The dashed line in Fig. 1(b) at τ_2 = 178 ns shows the duration of each of the CR pulses for the $ZX_{-\pi/2}$ gate for these data. The total $ZX_{\pi/2}$ gate length is, therefore, $2 \times \tau_2 + 2 \times 32 = 420$ ns. The equivalent gate length for the original CR scheme is shown in Fig. 1(a) at τ_1 = 356 ns.

We performed QPT on the 178 ns $ZX_{-\pi/2}$ gate (Fig. 2) by preparing an overcomplete set of 36 states generated by $\{I, X_\pi, X_{\pm\pi/2}, Y_{\pm\pi/2}\}$, applying the gate to each of them and performing state tomography. We use the Pauli basis to represent QPT through the Pauli transfer matrix $\mathcal{R}$ [17]. The raw data are post-processed with a semidefinite algorithm [17] to take into account physicality constraints such as complete positivity and trace preservation of the process. We obtain a gate fidelity from the raw data of $F_g = 0.8830$ and a maximum-likelihood estimated fidelity of $F_{\text{mle}} = 0.8799$. These results, as the RB measurements described next suggest, are probably dominated by SPAM errors.

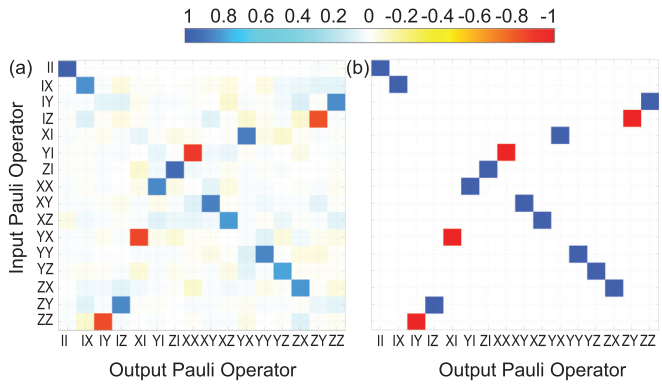

FIG. 2. (Color online) QPT of the $ZX_{-\pi/2}$ gate with τ_2 = 178 ns. (a) Experimentally extracted Pauli transfer matrix. The gate fidelity is $F_g = 0.8830$ raw and $F_{\text{mle}} = 0.8799$ after applying a maximum likelihood algorithm. (b) Ideal Pauli transfer matrix representation of the $ZX_{-\pi/2}$ gate.

We base our implementation of a two-qubit RB protocol on the theory described in Refs. [5] and [14]. We randomly choose a sequence $\{C_1, C_2, \ldots, C_{20}\}$ of 20 Cl gates from the two-qubit Cl group. From this sequence, we then construct a series of truncations $\{m_1, m_2, \ldots, m_{20}\}$, where $m_i = \{C_1, C_2, \ldots, C_i\}$. Each truncation is made self-inverting by adding a final pulse I_i which returns the system to the $|00\rangle$ state before readout. A whole RB experiment, therefore, consists of a series of pulse trains $\{N_1, N_2, \ldots, N_{20}\}$, where $N_i = \{m_i, I_i\}$.

The fidelity of the $|00\rangle$ state after each N_i, obtained by joint readout of the two qubits [28], can be fit to an exponential model $F(i, |00\rangle) = A\alpha^i + B$, and the average error rate per Cl operation is related to α by $r = 1 - \alpha - (1-\alpha)/d$, where $d = 2^n$ for n qubits [5]. In this model, SPAM errors are absorbed by the constants A and B and therefore the parameter α provides a SPAM-free estimation of the average error per Cl gate. This model, however, only gives an estimation of the average error per Cl operation.

We can modify the protocol in order to estimate the error of a particular Cl gate of interest, $\overline{C}$, as described in Refs. [13] and [14]. In the modified protocol, we construct similar random sequences of Cl gates as in the original implementation and then append (interleave) the gate $\overline{C}$ after each element in the sequence. A final inverting Cl gate is added at the end of each sequence truncation.

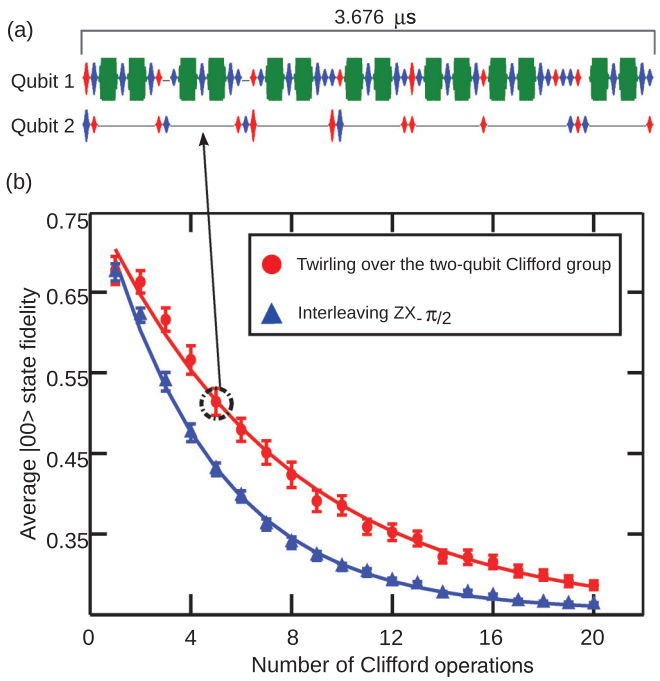

FIG. 3. (Color online) RB experiments on a two-qubit system. (a) Two-qubit pulse sequence for 5 Cl gates randomly selected from the two-qubit Cl group. Tall Gaussians represent π rotations, whereas short ones represent $\pi/2$ rotations. A final Cl gate is added to make the sequence self-inverting. (b) Fidelity decay for $|00\rangle$ in the standard (circles) and in the interleaved (triangles) RB protocols. The decays are fitted to an exponential model to extract an average error per Cl operation of $r = 0.0936 \pm 0.0058$ (standard protocol) and a $ZX_{-\pi/2}$ error of $r_C = 0.0653 \pm 0.0014$. The arrow shows the truncation that would correspond to the pulse sequence shown in (a) and which has an average $|00\rangle$ state fidelity of over 50%.

Figure 3(b) shows the average $|00\rangle$ state fidelity over random sequences of Cl gates with lengths ranging from 1 to 20 for both the standard (circles) and the interleaved (triangles) RB protocols. Each data point was averaged over 40 different random sequences. Both sets of RB data in Fig. 3(b) are well described by an exponential model, with reduced χ^2 values of 0.589 and 0.386 for the standard and interleaved RB protocols, respectively [29]. Our construction of the Cl group results in 30 $ZX_{-\pi/2}$ gates on average for a sequence of 20 Cl gates. The pulses of one particular sequence, comprising 7 two-qubit and 23 single-qubit gates, are shown in Fig. 3(a). In the case of the standard RB implementation experiment, we obtain $\alpha = 0.8752 \pm 0.0078$, which results in an average error per Cl operation of $r = 0.0936 \pm 0.0058$. For the interleaved experiment, $\alpha_C = 0.7990 \pm 0.0058$, from which r_C can be estimated as $r_C = (d-1)(1-\alpha_C/\alpha)/d = 0.0653 \pm 0.0014$ [13]. All errors here represent a 1σ confidence interval obtained from the Jacobian of the fitting model [15]. The average error per Cl operation for the single-qubit Cl group for each qubit was also measured, yielding $r_1 = 0.0041 \pm 0.0001$ for qubit 1 and $r_2 = 0.0048 \pm 0.0002$ for qubit 2 [20].

The effective coupling strength of the two qubits, given by the product $\epsilon(t)\mu$ multiplying the ZX interaction in Eq. (1), can be increased with the amplitude of the CR driving tone $\epsilon(t)$. Thus, larger driving amplitudes result in a faster evolution of the system and, therefore, faster oscillations in Fig. 1(b) and shorter τ_2. The ultimate limit for the speed of the $ZX_{-\pi/2}$ gate is determined by the frequency of the oscillations induced by the ZX term, the qubit-qubit detuning Δ, and the qubit anharmonicities. For the strongest drives, energy leakage into other levels in the system prevent the gate from becoming faster [16,30].

We applied the two-qubit RB protocol to our system for different $ZX_{-\pi/2}$ half-lengths, with τ_2 ranging from 115 to 800 ns. Figure 4 shows the average error per Cl operation as a function of τ_2 and the calculated coherence-limited average

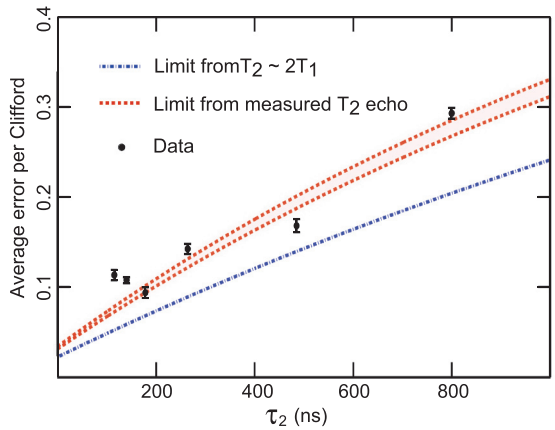

FIG. 4. (Color online) Average error per Cl operation as a function of the $ZX_{-\pi/2}$ half-gate length τ_2. An estimated error from the measured T_2 echo is shown as dashed lines, with an interval of confidence of 1σ represented by the shaded area. The estimated error for a coherence time equal to twice the qubit relaxation times (dash-dotted) is also plotted. Error bars in the data represent 1σ confidence intervals. These results suggest that our average gate error is currently limited by qubit coherence.

error for the measured T_2 echo of both qubits (dashed lines) and for $T_2^{(1,2)} = 2T_1^{(1,2)}$ (dash-dotted line), which imposes the gate error limit in the absence of dephasing noise. The shaded region delimits the uncertainty in the measured coherence time. We can see that, whereas most data points fell around the coherence-delimited error values, for the two shortest realizations of the $ZX_{-\pi/2}$ the RB experiments yielded an average error per Cl operation above the limit imposed by coherence times. This was probably due to leakage into higher qubit levels at high CR driving amplitudes and to the spurious off-resonance driving of the control qubit. For longer gates, the observed experimental values indicate that our $ZX_{-\pi/2}$ is essentially coherence-limited. We attribute the scattering of the data points in Fig. 4 to small variations in T_1 and T_2, which were observed to move by about 1 or 2 μs up or down for both qubits over the interval of 6–12 h, approximately equal to the amount of time taken to perform each RB protocol.

As a final demonstration of the robust repeatability of our $ZX_{-\pi/2}$ gate, we programed and ran a two-qubit Grover's algorithm [31] with an average algorithm fidelity of $\sim$80% across all four oracles. The result is consistent with the computed fidelity obtained from the product of the individual gate fidelities for the decomposed algorithm, consisting of two $ZX_{-\pi/2}$ gates and 16 single-qubit gates.

In conclusion, we have implemented a RB protocol on two superconducting qubits by using a robust implementation of an entangling two-qubit gate plus single-qubit unitaries. This gate pulse sequence echoes away single-qubit terms in the control Hamiltonian, which tend to be nonreproducible in long gate sequences. Our implementation allows the experimental realization of multiple repeated two-qubit gates on demand, as well as the complete two-qubit RB protocol in superconducting qubits. Furthermore, an interleaved RB experiment yields a gate fidelity of 0.9347, which compares favorably to the fidelity of 0.8799 obtained by QPT performed on the same gate. Our results show the importance of a protocol insensitive to SPAM errors, especially as the processes to benchmark become increasingly higher in fidelity. Measurements for different gate durations suggest that our gate is currently limited by the coherence time of our qubits. Nonetheless, with continuing progress in increased coherence times, fixed-frequency superconducting qubits are primed to perform longer and more complex quantum computations.

We acknowledge discussions and contributions from B. Johnson, C. Ryan, S. Merkel, E. Lucero, and D. McClure. We acknowledge use of the Cornell NanoScale Facility, a member of the National Nanotechnology Infrastructure Network, which is supported by the National Science Foundation (Grant No. ECS-0335765). We acknowledge support from IARPA under Contract No. W911NF-10-1-0324. All statements of fact, opinion, or conclusions contained herein are those of the authors and should not be construed as representing the official views or policies of the US Government.

[1] J. F. Poyatos, J. I. Cirac, and P. Zoller, Phys. Rev. Lett. **78**, 390 (1997).
[2] I. Chuang and M. Nielsen, J. Mod. Opt. **44**, 2455 (1997).
[3] J. Emerson, R. Alicki, and K. Zyczkowski, J. Opt. B **7**, S347 (2005).
[4] E. Knill *et al.*, Phys. Rev. A **77**, 012307 (2008).
[5] E. Magesan, J. M. Gambetta, and J. Emerson, Phys. Rev. Lett. **106**, 180504 (2011).
[6] M. J. Biercuk *et al.*, Quantum Inf. Comput. **9**, 0920 (2009).
[7] K. R. Brown *et al.*, Phys. Rev. A **84**, 030303 (2011).
[8] C. Ryan, M. Laforest, and R. Laflamme, New J. Phys. **11**, 013034 (2009).
[9] J. M. Chow *et al.*, Phys. Rev. A **82**, 040305 (2010).
[10] J. M. Chow *et al.*, Phys. Rev. Lett. **102**, 090502 (2009).
[11] H. Paik *et al.*, Phys. Rev. Lett. **107**, 240501 (2011).
[12] S. Olmschenk *et al.*, New J. Phys. **12**, 113007 (2010).
[13] E. Magesan *et al.*, Phys. Rev. Lett. **109**, 080505 (2012).
[14] J. P. Gaebler *et al.*, Phys. Rev. Lett. **108**, 260503 (2012).
[15] J. M. Gambetta *et al.*, Phys. Rev. Lett. **109**, 240504 (2012).
[16] J. M. Chow *et al.*, Phys. Rev. Lett. **107**, 080502 (2011).
[17] J. M. Chow *et al.*, Phys. Rev. Lett. **109**, 060501 (2012).
[18] L. M. K. Vandersypen and I. L. Chuang, Rev. Mod. Phys. **76**, 1037 (2007).
[19] S. Aaronson and D. Gottesman, Phys. Rev. A **70**, 052328 (2004).
[20] See Supplemental Material at http://link.aps.org/supplemental/10.1103/PhysRevA.87.030301 for additional information on the two-qubit Cl group and the qubits experimental parameters.
[21] Our procedure is equivalent to that of Ref. [14] and finds the same average number of two-qubit gates per Cl operation.
[22] A. Blais, R. S. Huang, A. Wallraff, S. M. Girvin, and R. J. Schoelkopf, Phys. Rev. A **69**, 062320 (2004).
[23] R. Barends *et al.*, Appl. Phys. Lett. **99**, 113507 (2011).
[24] A. D. Córcoles *et al.*, Appl. Phys. Lett. **99**, 181906 (2011).
[25] G. S. Paraoanu, Phys. Rev. B **74**, 140504 (2006).
[26] C. Rigetti and M. Devoret, Phys. Rev. B **81**, 134507 (2010).
[27] F. Motzoi, J. M. Gambetta, P. Rebentrost, and F. K. Wilhelm, Phys. Rev. Lett. **103**, 110501 (2009).
[28] J. Majer *et al.*, Nature (London) **449**, 443 (2007).
[29] The reduced χ^2 values [15] depend strongly on estimates of the standard deviation of the underlying distribution. In our experiments, the data do not always appear normally distributed when clustered around unit fidelity and therefore the reduced χ^2, dominated by only a few points, is significantly less than unity.
[30] P. C. de Groot *et al.*, New J. Phys. **14**, 073038 (2012).
[31] L. K. Grover, Phys. Rev. Lett. **79**, 325 (1997).